International Journal of Modern Nonlinear Theory and Application, 2025, 14(4), 74-95
https://www.scirp.org/journal/ijmnta
ISSN Online: 2167-9487
ISSN Print: 2167-9479

Computational Analysis of Single-Sided Ventilation for a Cubic Room in Dhaka City with the Influence of Solar Radiation

Golam Mostafa

Department of Computer Science and Engineering, Southeast University, Dhaka, Bangladesh
Email: golam.mostafa@seu.edu.bd

How to cite this paper: Mostafa, G. (2025) Computational Analysis of Single-Sided Ventilation for a Cubic Room in Dhaka City with the Influence of Solar Radiation. *International Journal of Modern Nonlinear Theory and Application*, **14**, 74-95.
https://doi.org/10.4236/ijmnta.2025.144005

Received: October 1, 2025
Accepted: November 23, 2025
Published: November 26, 2025

Abstract

Energy consumption in Bangladesh has been increasing day by day due to population growth, industrial, and technological development. In accordance with the annual report of the Bangladesh Power Development Board (BPDB), the domestic sector is the largest energy-consuming sector in Bangladesh. The average monthly temperature of Dhaka city is moving forward, according to the Bangladesh Meteorological Department. The rising numbers of different electrical appliances for cooling are responsible for this large energy consumption. In a living room, solar radiation has an essential influence on the heat balance in several ways. So, the use of natural ventilation with solar radiation in buildings is now a demand of the time. This study aims to examine the wind profiles and temperature distributions inside and outside the building to understand the indoor air quality as well as thermal comfort. In this research, a single room with single/double opening(s) on the windward wall and the leeward wall with the effect of solar radiation have been studied by using Computational Fluid Dynamics (CFD) based on the Finite Element Method (FEM). The standard k-ε turbulence model has been used in the present investigation on wind-driven natural ventilation with a three-dimensional room for four physical models, which have been calculated in the context of weather in Dhaka city. The physical model has been solved by the commercial software COMSOL Multiphysics. Based on wind direction, the output of airflow, ventilation rate, and average room temperature inside the room are approximately 0.4 m/s, 5.4×10^{-4} m^3/s and 300 K, respectively. The radiosity of the computational domain is in the range from 353 to 405 at noon. All values are satisfied with the ASHRAE standard for all configurations. Based on the data of air quality and the volume average temperature, double openings in the windward wall are more comfortable than the other openings. This outcome can open a new dimension in the field of an energy-efficient building to live healthily and reduce the consumption of the mechanical system and also help the designer to design buildings for considering the environmental parameters to build an energy-efficient city.

Keywords

Natural Ventilation, Solar Radiation, CFD, FEM, Turbulence Model

1. Introduction

World energy consumption has been increasing rapidly for the last decades, mainly due to population growth and industrial and technological development. According to the Energy Information Administration [1], energy consumption in buildings accounts for more than 40% of the primary energy consumption. Now, the heat balance of a living room is inevitable from the energy consumption and the possible effect of solar radiation. Therefore, vast changes have to be made in the building sector, especially in the Heating, Ventilation, and Air-Conditioning (HVAC) systems, in order to reach the aforementioned targets. By reducing the need for electrical equipment and other cooling systems, energy can be saved and thus comfortable living environment can be enhanced. Kusuda [2] described the relationship between heating and cooling load calculation, which is a starting point for building energy consumption analysis and equipment sizing. Jiang *et al.* [3] investigated the mechanism of natural ventilation driven by wind force, Large-Eddy Simulation (LES). In the meanwhile, detailed airflow fields, such as mean and fluctuating velocity and pressure distribution inside and around building-like models, were measured by wind tunnel tests and compared to LES results for model validation. Three ventilation cases, single-sided ventilation with an opening in the windward wall, single-sided ventilation with an opening in the leeward wall, and cross ventilation, are studied. Allocca *et al.* [4] studied single-sided natural ventilation by using a Computational Fluid Dynamics (CFD) model, together with analytical and empirical models. The CFD model was applied to determine the effects of buoyancy, wind, or the combination of ventilation rates and indoor conditions. Jiang and Chen [5] investigated buoyancy-driven single-sided natural ventilation with large openings. Detailed airflow characteristics inside and outside of the room and the ventilation rate were measured. Seifert *et al.* [6] investigated a single-zone cubic building with two equal large openings using a computational fluid dynamics approach. They analyzed the driving forces and the ventilation flow rates due to wind as a function of the geometry, size, and relative location of the two openings. The ventilation flow rates are found to be affected by both wind flows around and through the building when the two openings are relatively large. Evola and Popov [7] applied the Reynolds Averaged Navier-Stokes (RANS) equation to wind-driven natural ventilation in a cubic building. They determined the ventilation rate for single-sided and cross ventilation using the k-ε turbulence model and Renormalization Group (RNG) theory and compared the results. Larsen and Heiselberg [8] analyzed the wind direction, which is an important parameter for single-sided ventilation. They also show that single-sided ventilation depends on the size, type, and location of the opening. Bangalee *et al.* [9] considered a building with multiple windows to investigate the wind-driven ventilation system using Computational Fluid Dynamics (CFD), whose acceptance and accuracy are growing very fast. The Renormalization Group (RNG) k-ε turbulence model is chosen to simulate cross and single-sided ventilation with a specified accuracy after validating the methodology through a satisfactory comparison with an experimental result. Montazeri and Blocken [10] presented a systematic evaluation of 3D steady Reynolds-Averaged Navier-Stokes (RANS) CFD for predicting mean wind pressure distributions on the windward and leeward surfaces of a medium-rise building with and without balconies. It is shown that building balconies can lead to very strong changes in wind pressure distribution. Idris and Huynh [11] analyzed the air velocities in a single-sided naturally ventilated room along with an atmospheric zone into four different window locations and predicted air distribution inside the room. Gendelis and Jakovics [12] considered the heat balance of a room and its dependence on solar radiation and ventilation conditions. They analyzed the physical parameters of thermal comfort conditions, the airflow velocities, indoor temperatures, and their gradients. The distributions are calculated according to the solar radiation source through the window and the pressure difference between the opposite walls.

In Bangladesh, the annual report 2018-2019 of Bangladesh Power Development Board [13] showed that the domestic sector is the largest energy consumption sector and it is increasing day by day. Ahmmad [14] analyzed the Wind Resources for Energy Production in Bangladesh. He estimated the wind power density, the annual mean wind power, and the annual mean wind speed. Hossain *et al.* [15] analyzed the pattern of change of temperature of Dhaka city using the data of maximum and minimum monthly temperature of 1995-2010 period collected from the Bangladesh Meteorological Department. This study reveals that the minimum average monthly temperature is showing a significant increasing pattern. In comparison to experimental investigation, temperature and average turbulent airflow distributions in the 2D and 3D models of a living room are modeled. It is shown that solar radiation has an essential influence on the heat balance of the room in a number of ways and on thermal comfort in the room. Computational Fluid Dynamics (CFD) is cost-effective and easy to investigate the flow due to the change of geometry. So, it is the demand of time to use the powerful tool CFD to model natural ventilation in buildings with solar radiation.

As the structure is distributed, the initial discussion is provided in the introductory that contains the fundamental idea of this work; the 2D and 3D physical models of the computational domain with a cubic building are discussed in the second section; the governing equations, boundary conditions, meshing of the physical models and the justification of the proposed methodology are provided in the third section; the discussion of the attained results and graphical representations are presented in the fourth section which contains velocity and temperature distribution, ventilation rate, and rediosity; and the conclusive overview of this work is provided in the last section.

2. Physical Models

An important factor to select the site and building for simulation is the climatic characteristics. The climatic characteristics of Dhaka City differ from other cities of the country due to its location and rapid physical development in last few decades. Physical and environmental characteristics are further modified in different locations within the city. This is due to the density of built environment, building types, building heights and orientations, surface quality of the area—whether hard or soft, depending on vegetal cover and presence of water bodies and ponds—materials used for construction, and other related factors. The criteria for site and building selection to determine the typical example office space were based on urban boundary, trend of typical office design, Building Construction Regulations of the City Authority, internal layout for daylight inclusion and distribution and scale and volume of the building.

In this study, single-sided natural ventilation has been presented for windward and leeward cases of three-dimensional model. Physical processes in a room with different heights and different locations of windows are modelled using specialized Computational Fluid Dynamics (CFD). Calculations are carried out in an empty room without any human or mechanical activity and compared with previous experimental measurements. Numerical analysis has shown distinct relationship between room dimensions (height in this case) and state of comfort in the room. The single-sided ventilation with opening(s) on the windward wall and leeward is considered. In this research, four different cases are considered and the cases are:

Case 1: single-sided ventilation with an opening on the windward wall;

Case 2: single-sided ventilation with an opening on the leeward wall;

Case 3: single-sided ventilation with double openings on the windward wall;

Case 4: single-sided ventilation with double openings on the leeward wall.

The positions of the single opening (Case 1 and Case 2) and double openings (Case 3 and Case 4) are considered on lower and middle of the building respectively. In this study, a cubic building is considered whose walls are made of concrete. The dimension of the building-like model is 250 mm × 250 mm × 250 mm.

Two different building models are used: the first one is provided with a door-like opening sized 90 mm × 100 mm (width × height) for Case 1 and Case 2, and the second one is provided with window-like double openings, both of them are sized 90 mm × 50 mm (width × height) for Case 3 and Case 4. All cases are used to study single-sided wind-driven ventilation. The thickness of the walls is 5 mm in both building models. Figure 1 shows a schematic view of the building model. Furthermore, a logarithmic wind profile upwind of the building is considered in Figure 2. The dimension of the computational domain, 3.25 m × 2.25 m × 1 m, displayed in Figure 3, is chosen large enough in order not to disturb the air flow around the building. Three-dimensional view of the location and arrangement of the opening(s) of a cubic building for windward wall and leeward wall are shown in Figure 4 and Figure 5 respectively.

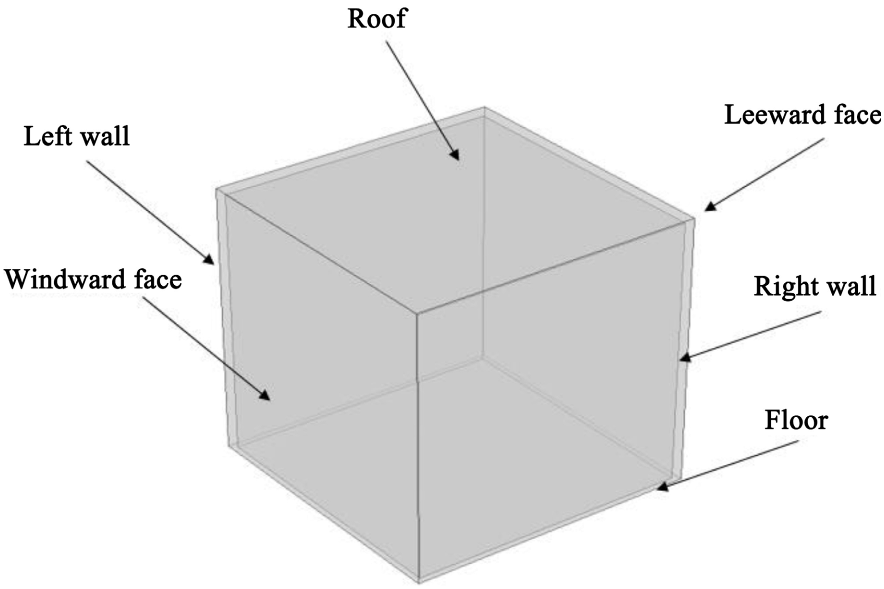

Figure 1. Schematic view of the building model.

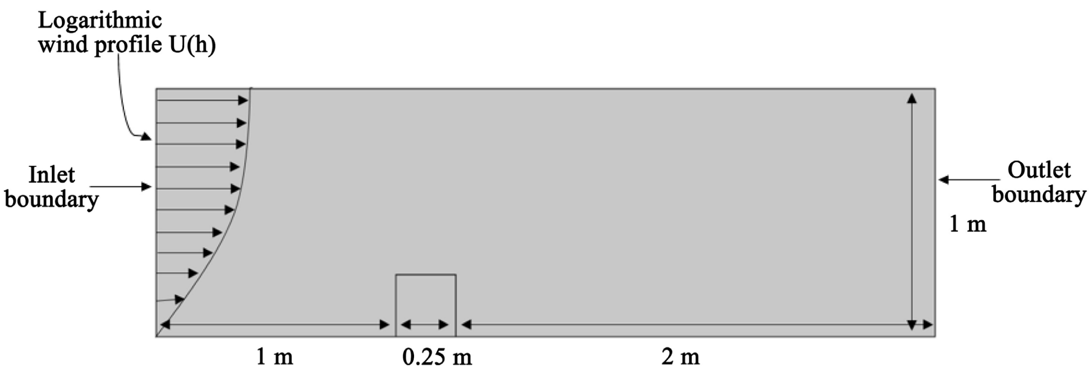

Figure 2. Two-dimensional (2D) view of the computational domain and logarithmic wind profile.

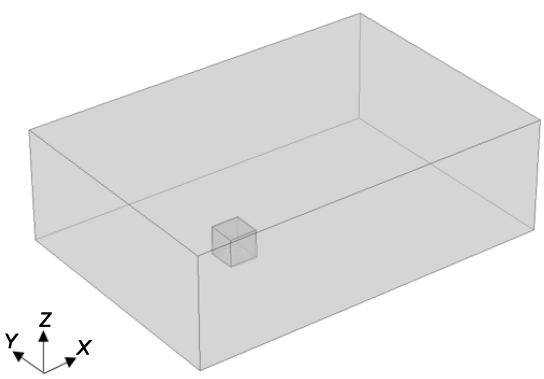

Figure 3. Three-dimensional (3D) view of the computational domain.

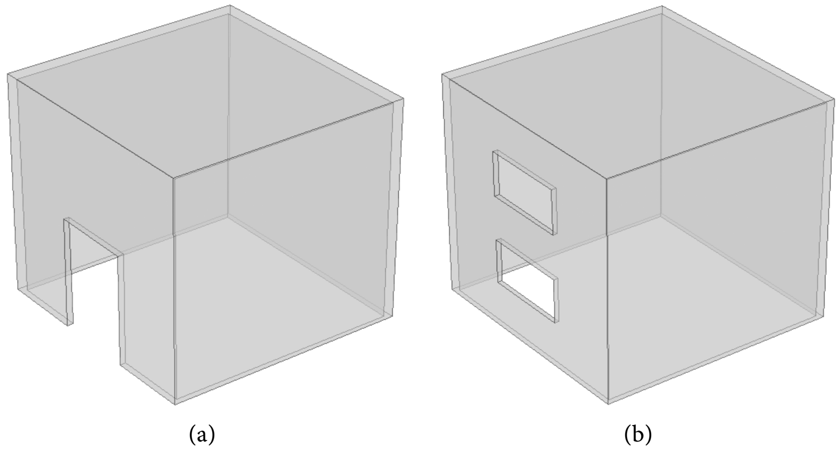

Figure 4. 3D view of the location and arrangement of the opening(s) for windward face ((a) Case 1; (b) Case 3).

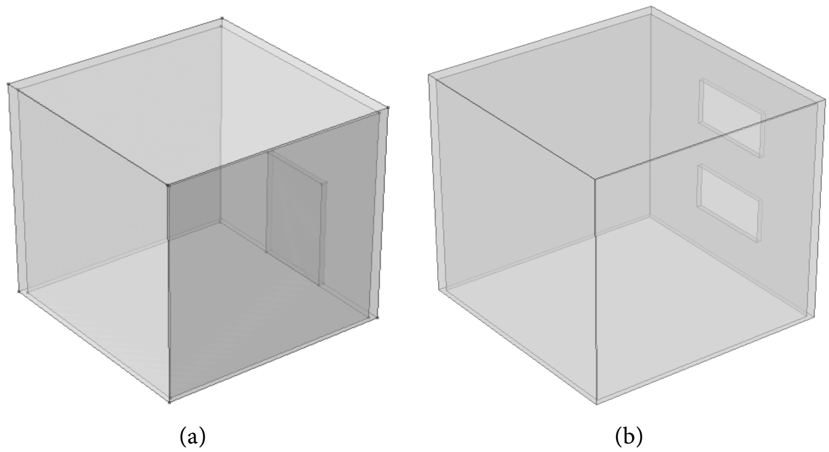

Figure 5. 3D view of the location and arrangement of the opening(s) for leeward face ((a) Case 2; (b) Case 4).

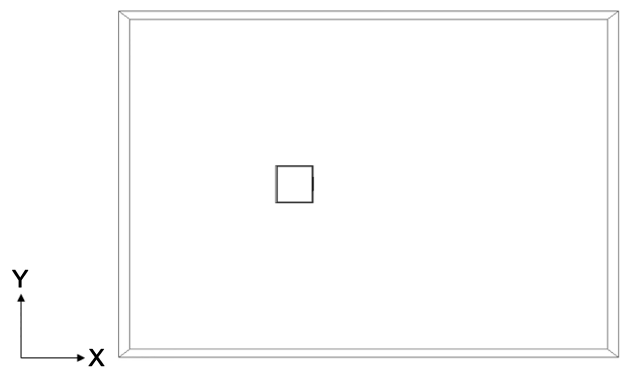

Figure 6. Computational domain (3D view of *xy*-plane).

Figure 6 shows the three-dimensional view of computational domain's *xy*-plane. Since wind-driven ventilation depends on pressure difference, so physical model is a very important factor for natural ventilation. In this study, detailed physical models are prepared to calculate the wind flow, temperature, radiosity, and ventilation rate.

3. Mathematical Model

Outdoor environment depends on natural forces. It is difficult to control and measure these unpredictable forces. A tool is needed that will enable designers to easily manipulate a building's design in order to observe trends and evaluate various potential designs. Full-scale tests [16], wind tunnel tests [8], and computational techniques are common procedures in studying a building and its surrounding outdoor environment. The full-scale test and wind tunnel test are usually time-consuming, expensive, and also may not be capable of capturing whole field information since there can only be a limited number of measuring points. The development of Computational Fluid Dynamics (CFD) [17]-[21] allows the investigation of building wind environments, enabling the study of entire detailed flow fields in a timely and cost-effective manner. So, CFD is a powerful tool for getting information about the air flow and pressure distribution around and inside the buildings. CFD is a branch of fluid mechanics that uses numerical methods and algorithms to solve and analyze problems that involve fluid flows. Its application becomes more and more popular as the computational power and technology have been increased and improved the turbulence modelling. Among the techniques studied by Chen, he agrees that CFD seems to be one of the most attractive techniques for building environment design, since it is the most affordable, accurate, and informative method [22].

The common CFD techniques are Direct Numerical Simulation (DNS), Large-Eddy Simulation (LES) and Reynolds Averaged Navier-Stokes (RANS) equation with turbulence models. Each technique handles turbulence in different ways [23]. Among those techniques, RANS is widely used by most CFD software [24]. RANS solves the time-averaged Navier-Stokes equations by using approximations to simplify the calculation of turbulence flow. The present investigation will be focused on the application of three-dimensional RANS modelling on wind-driven natural ventilation of opening(s) at single-sided buildings.

3.1. Governing Equations

The Navier-Stokes equations represent the fundamental governing equations for fluid flow. The incompressible Navier-Stokes equations in conservation form are

$$\frac{\partial U_i}{\partial x_i} = 0$$

$$\frac{\partial U_i}{\partial t} + U_j \frac{\partial U_i}{\partial x_j} = -\frac{1}{\rho}\frac{\partial P}{\partial x_i} + \frac{\partial}{\partial x_j}\left[v\left(\frac{\partial U_i}{\partial x_j} + \frac{\partial U_j}{\partial x_i} \right) + \tau_{ij} \right]$$

The quantity $\tau_{ij} = -\overline{u_i' u_j'} = v_t\left(\frac{\partial U_i}{\partial x_j} + \frac{\partial U_j}{\partial x_i} \right) - \frac{2}{3} K \delta_{ij}$ is known as the Reynolds stress tensor, which is symmetric and v_t is the kinetic eddy viscosity assumed as an isotropic scalar quantity.

$$\frac{\partial U_i}{\partial t}+U_j\frac{\partial U_i}{\partial x_j}=-\frac{1}{\rho}\frac{\partial P}{\partial x_i}+\frac{\partial}{\partial x_j}\left[\nu\left(\frac{\partial U_i}{\partial x_j}+\frac{\partial U_j}{\partial x_i}\right)+\nu_t\left(\frac{\partial U_i}{\partial x_j}+\frac{\partial U_j}{\partial x_i}\right)-\frac{2}{3}K\delta_{ij}\right]$$

In radiation problems, the conservation of energy is given by

$$\frac{\partial T}{\partial t}+U_j\frac{\partial}{\partial x_j}(T)=\frac{k}{\rho C_p}\frac{\partial^2}{\partial x_i^2}(T)+\frac{1}{\rho C_p}\dot{Q}_i$$

where T is the temperature of the fluid, k is the thermal conductivity, C_p is the specific heat of the fluid at constant pressure and $\dot{Q}_i$ is the net heat transfer from surface i.

Radiation heat transfer between surfaces depends on the orientation of the surfaces relative to each other as well as their radiation properties and temperatures. Consider an enclosure consisting of N black surfaces maintained at specified temperatures. For each surface i, we can write

$$\dot{Q}_i=\sum_{j=1}^{N}\dot{Q}_{ij}=\sum_{j=1}^{N}A_iF_{ij}\sigma\left(T_i^4-T_j^4\right)$$

where A_i is surface area and F_{ij} indicates the fraction of the radiation leaving surface i that strikes surface j directly.

In this study, non-black surfaces are considered. In an *N*-surface enclosure, the conservation of energy principle requires that the net heat transfer from surface *i* to be equal to the sum of the net heat transfers from *i* to each of the *N* surfaces of the enclosure.

$$\dot{Q}_i=\sum_{j=1}^{N}\dot{Q}_{ij}=\sum_{j=1}^{N}\frac{J_i-J_j}{R_{ij}}$$

where $R_{ij}=\frac{1}{A_iF_{ij}}$ is called the space resistance to radiation and J_i and J_j are the radiosity for the surface i to j. The standard *k*-*ε* turbulence model was used in this study because the flow is fully turbulent and the effects of molecular viscosity are negligible [7]. The turbulent kinetic energy, k, and its rate of dissipation, ε, in the flow field are calculated from two additional transport equations. The model transport equation for k is derived from the exact equation, while the model transport equation for ε was obtained using physical reasoning and bears little resemblance to its mathematically exact counterpart. The *k*-*ε* transport equations [7] are:

$$\frac{\partial k}{\partial t}+U_j\frac{\partial k}{\partial x_j}=\frac{\partial}{\partial x_j}\left[\left(\nu+\frac{\nu_t}{\sigma_k}\right)\frac{\partial k}{\partial x_j}\right]+\frac{1}{\rho}P_k-\varepsilon$$

$$\frac{\partial \varepsilon}{\partial t}+U_j\frac{\partial \varepsilon}{\partial x_j}=\frac{\partial}{\partial x_j}\left[\left(\nu+\frac{\nu_t}{\sigma_\varepsilon}\right)\frac{\partial \varepsilon}{\partial x_j}\right]+C_{\varepsilon 1}\frac{\varepsilon}{k\rho}P_k-C_{\varepsilon 2}\frac{\varepsilon^2}{k}$$

where P_k is the production rate of turbulent kinetic energy, which depends on the turbulent viscosity and the velocity distribution. In **Table 1**, the values of all the parameters used by COMSOL Multiphysics are provided.

Table 1. Constants for the turbulence model.

Constants	Values
C_μ	0.09
$C_{\varepsilon 1}$	1.44
$C_{\varepsilon 2}$	1.92
σ_K	1.0
σ_ε	1.3

3.2. Boundary Conditions

In this study, the CFD software based on the finite element method (Galerkin weighted residual method) has been used to solve the set of equations provided by k-ε models. In the case of vertical wind direction, the computational domain was constructed that had a height of $4H$, width of $9H$ and length of $13H$ where $H = 0.25\text{ m}$. The ability to accurately model outdoor airflow around buildings is necessary to provide the correct boundary conditions for the indoor building environment that is naturally ventilated. As far as the boundary conditions are concerned, at the inlet of upwind boundary, a logarithmic profile of the stream wise velocity component U has been applied: $U(h) = \frac{U_0}{K}\ln\left(\frac{h}{h_0}\right)$; where h is the distance from the ground, $K = 0.41$ is the Von Karman's constant, U_0 and h_0 have been determined through the best fit of the available data and experimental data. The velocity components along with vertical and span wise direction were equated to zero. In addition, as the distribution of k and ε on the inlet boundary was unknown, the following relations have used: $k = \frac{3}{2}\left(U_{avg} \cdot T_i^2\right)$; $\varepsilon = c_\mu^{3/4}\frac{k^{3/2}}{l_t}$; where U_{avg} is the average flow velocity, T_i is the turbulence intensity and l_t is the turbulence length scale. To solve turbulence conditions, $T_i = 1\%$ [25] and $l_t = 0.4\text{ m}$ [7] have been used in this research. A constant pressure is assumed at the outlet of the computational domain, while the gradients of all the dependent variables are assumed to vanish. The ambient conditions at the domain boundary were represented by specifying ambient pressure of 1 atm and temperature of 33˚C. For all cases, 33˚C heated air entered into the region through the inlet. Standard wall functions were used and the no-slip velocity boundary condition was applied for the fluid-wall interaction. The wall of the room is modelled as heat-transmitting concrete material with emission $\varepsilon = 0.85$. All objects except the transparent window are modelled as grey bodies. Owing to the ellipticity of the earth's orbit, the actual solar constant changes throughout the year within ±3.4%. As a result, the solar radiation reaching the earth's surface is about 950 W/m^2 on a clear day and much less on a cloudy day, in the wavelength band 0.3 to 2.5 μm. The thermal expansion coefficient of the air is based on the ambient temperature. The commercial software COMSOL Multiphysics 5.2 based on finite element method is used for computation.

3.3. Meshing of the Physical Models

Physics-controlled mesh is prepared using COMSOL Multiphysics Meshing. The element sizes for this meshing are different, such as fine, extra fine, extremely fine, finer, coarse, coarser, extra coarse, extremely coarse, and normal. The number of mesh depends on different mesh types and element sizes. In 2D elements, triangular and rectangular are used and tetrahedral, Pyramidal, Prismatic and hexahedral are used for 3D elements. Table 2 shows that extremely coarse is suitable to use in this study. Total number of mesh for 3D cases is around 35,000 - 40,000, whereas 1800 - 2300 for 2D cases. In Figure 7, the computational domain is meshing with total number of elements around 35,000 to 40,000.

Table 2. The ventilation rate and processing time for different meshing.

Meshing	Ventilation Rate and Processing Time Calculation	
	Ventilation Rate (m^3/s)	Processing Time (s)
Coarse	0.0017	2000
Extremely Coarse	0.00145	4900
Finer	0.00135	30000

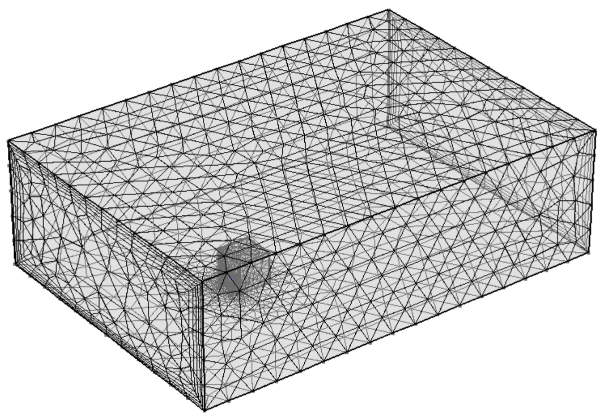

Figure 7. Meshing of windward wall with an opening (Case 1).

3.4. Code Validation

Wind-driven single-sided ventilation experiments were performed in the present study. In this validation study, CFD has been used to analyze single-sided ventilation by studying wind-driven windward flow through double opening. A single-sided ventilation experiment was used to validate the CFD model [11]. For the CFD simulation, the building model was set up and placed within a larger computational domain. After setting up the CFD model according to the experimental setup, the simulation was performed. In Figure 8, three vertical lines in the middle section of the domain A, B, and C are identified. Locations A and C have been chosen in order to describe the flow pattern close to the openings.

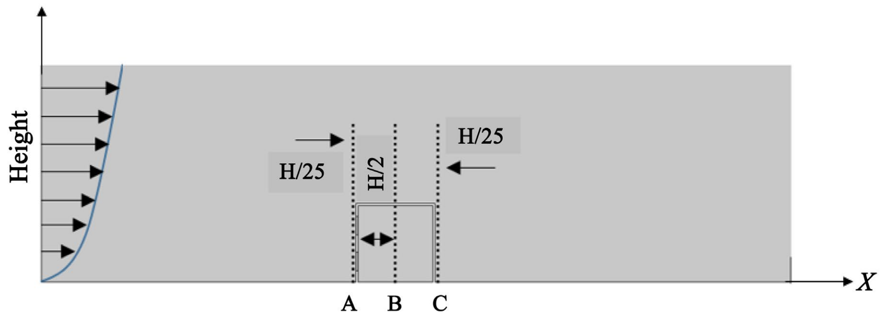

Figure 8. Location of the vertical lines.

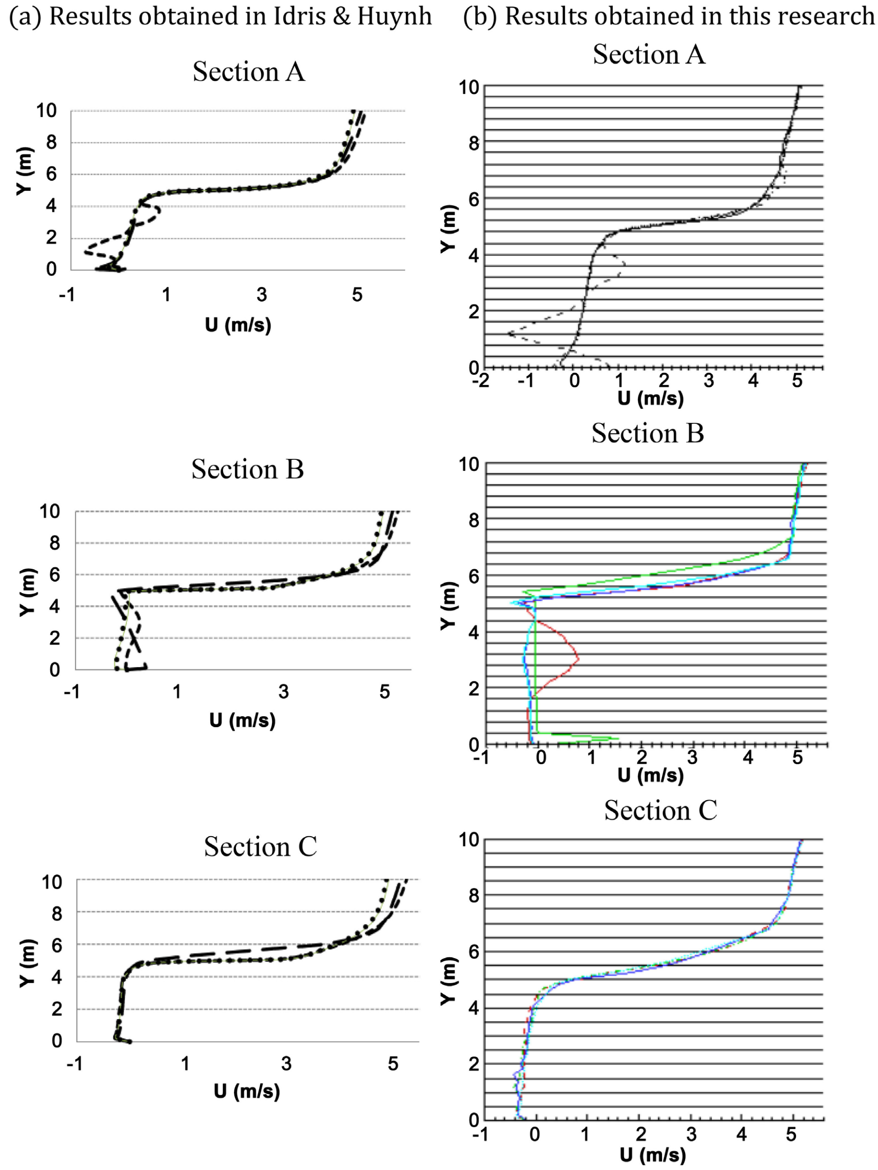

Figure 9. Code validation of the experimental model.

The velocity components have been determined, along streamwise and vertical direction, respectively. The third velocity component in x-axis has been neglected as it is supposed to be zero, due to the symmetry of domain. Figure 9(a) and Figure 9(b) show the velocity field results for the experiment model and CFD modeling results respectively, at every section of the building. The plots of Figure 9 show the vertical distribution of *x*-direction velocity *U* for ventilation patterns evaluated. Table 3 shows the mean absolute error analysis of velocity distribution of cubic room. From these validation cases, it is clear that the agreement between experimental results and CFD modeling for the interaction between outdoor and indoor flow in single-sided ventilation is very good.

Table 3. Mean absolute error analysis of velocity distribution of cubic room.

Section	Mean Absolute Error Analysis			
	Experimental Value	Predicted Value	Absolute Error	Mean Absolute Error
Section A	0.45 m/s	0.50 m/s	0.05	
Section B	−0.15 m/s	−0.13 m/s	0.02	0.027
Section C	−0.21 m/s	−0.20 m/s	0.01	

4. Results and Discussion

The present investigation will focus on the application of three-dimensional RANS modeling on natural ventilation of single/double opening(s) at the windward wall and the leeward walls of the single-sided building. The size of the domain is an important matter, especially for modeling airflow in buildings, because the realistic representation of ambient and external airflow is essential. It is necessary to consider a small computational domain with less number of grids to minimize the computational time. Airflow is mandatory for all three-dimensional models. It must ensure that the airflow is free from all kinds of hindrances in the outer domain for all cases.

4.1. Velocity Distribution

The aim of this study is to examine the wind profiles inside and outsides of the buildings through single/double opening(s). In this study, four physical models have been used in context of weather of Dhaka city. To compare with others results, three vertical lines are considered (from A to C), shown in Figure 8. Meteorological wind speeds are varying from 2 - 4 m/s in Dhaka city. Initially, at a low 2 m/s wind speed, buoyancy effects were dominant and consequently drove air in through the lower opening and out through the upper opening. At a wind speed of 4 m/s, this buoyancy effect diminished as the wind-driven force through the upper opening increased. The buoyancy and wind forces were approximately equal at this wind speed, resulting in the minimum ventilation rate over the range of wind speed.

In this analysis, the flow pattern inside the building as well as computational domain for all cases are considered. To show the flow pattern, air flow distribution and velocity distribution are essential. Figures 10-14 show the air flow distribution and velocity distribution in computational domain and cubic building for all cases at 3rd second. It was observed that the velocities change from time to time. After a few seconds, the changes are going to come down, which is approximately 3 seconds at that time-dependent results bear a physical resemblance to steady. Air flow distribution and stream lines are almost same. Since, after 3rd second, the changes are not worth watching, so the vertical velocity is calculated for 3rd second. Section-based comparison of streamwise velocity and vertical velocity for 3rd second is shown in **Figure 10** and **Figure 11** respectively. In computational domain, the behavior of streamwise velocity distribution for all cases is shown in **Figure 12**. The difference is evident in the regions close to horizontal surfaces. **Figure 13** shows the velocity distribution for all cases in *xy*-plane at time (t) = 3 sec. It is interesting to notice that leeward ventilation seems to produce an air movement inside the enclosed space more significant than windward ventilation, especially in the region close to the opening. In the windward single opening (Case 1), the air enters into the upper side of the opening and comes out through the lower side of that opening, but for the leeward single opening (Case 2), the air enters into the lower side of the opening and comes out through the upper side of that opening. Also, in the windward double openings (Case 3), the air enters into the upper opening

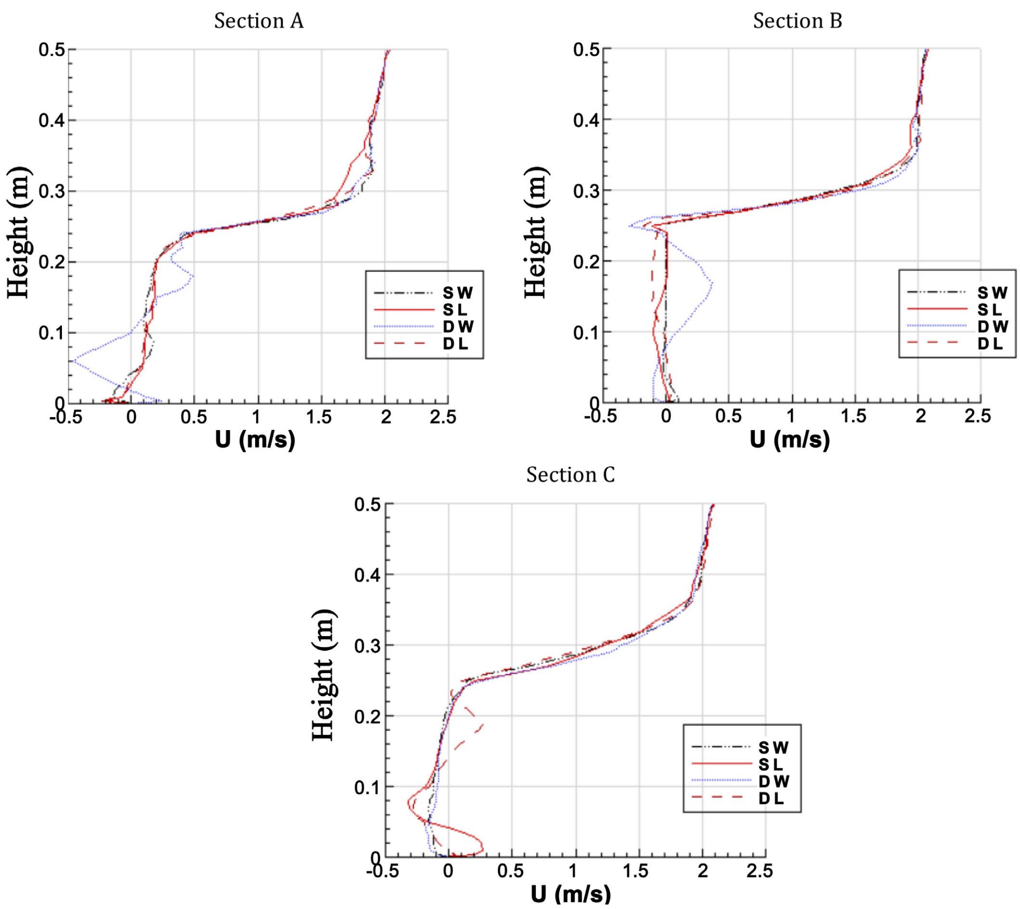

Figure 10. Streamwise velocity distribution for all cases (Case 1: S W, Case 2: S L, Case 3: D W, Case 4: D L) at $t = 3\text{ s}$.

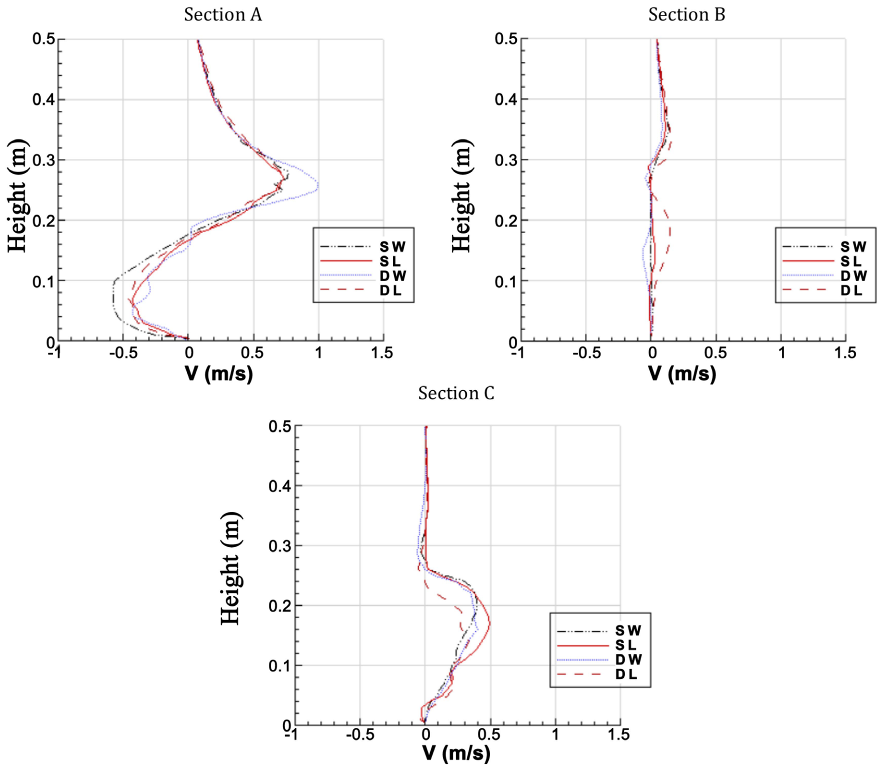

Figure 11. Vertical velocity distribution for all cases (Case 1: S W, Case 2: S L, Case 3: D W, Case 4: D L) at $t = 3\text{ s}$.

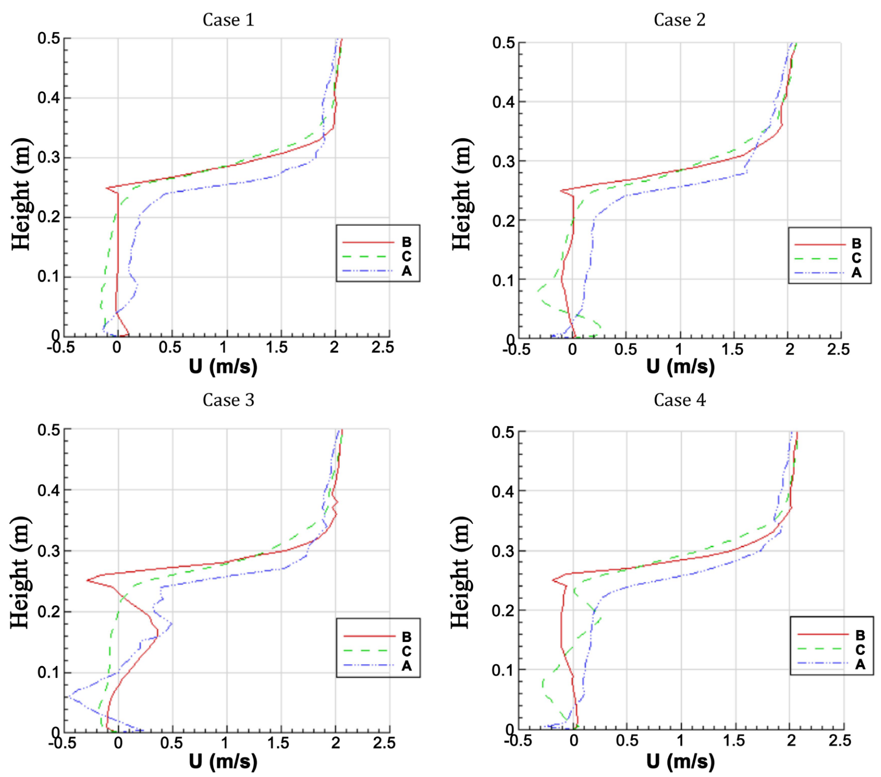

Figure 12. Velocity distribution for all cases in computational domain (Dash dot line: Section A, Solid line: Section B, Dashed line: Section C) at $t = 3\text{ s}$.

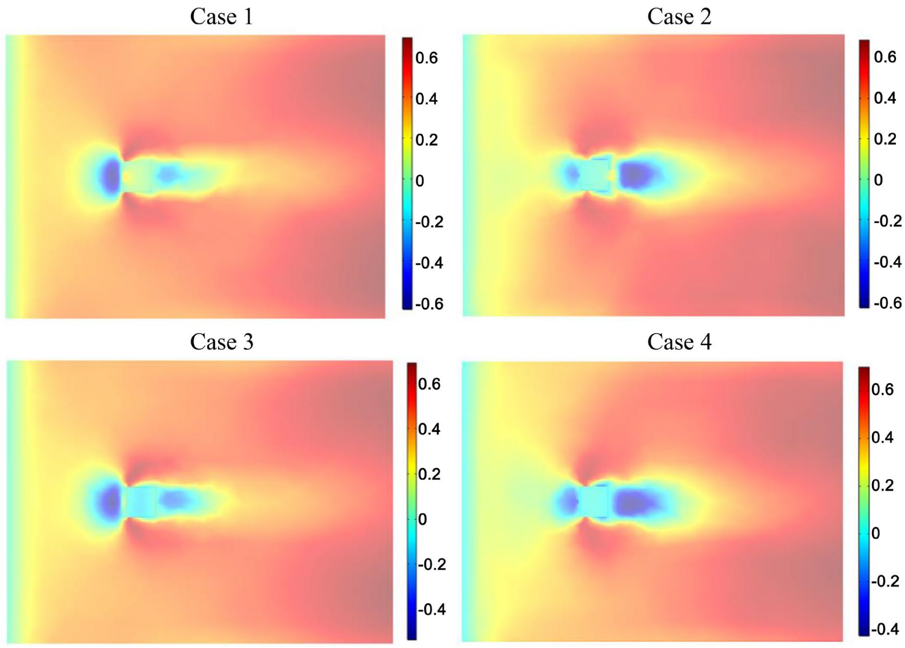

Figure 13. Velocity distribution for all cases in *xy*-plane at $t = 3\text{ s}$.

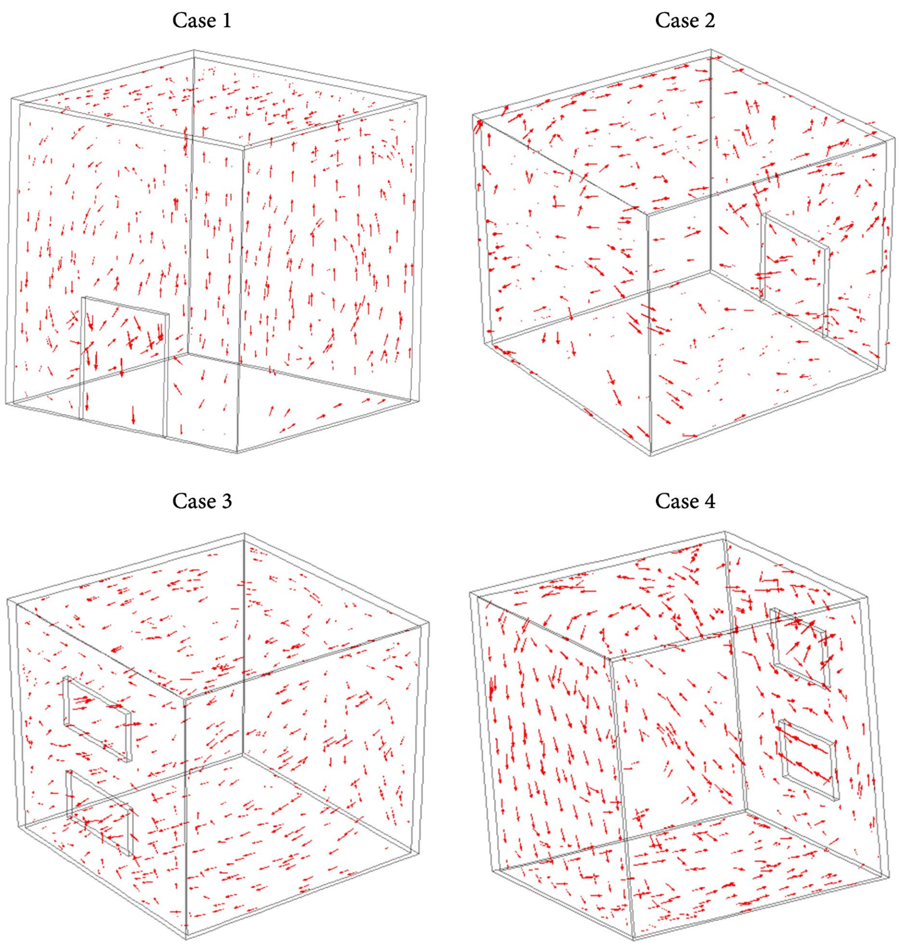

Figure 14. Air flow distribution in cubic building for all cases at $t = 3\text{ s}$.

and comes out through the lower opening, but for the leeward double openings (Case 4), the air enters into the building through the lower opening and comes out through the upper opening. Figure 14 shows the air flow distribution of the cubic room.

Above the roof of the building (height > 0.25), the velocity components U and V for all cases are similar in every section but in the cubic building, directions and velocity components are some disagreements in few sections. To choose the location of the opening(s) and description of the velocity profile inside the building and near the openings is the main purpose of this study. All the numerical results have been obtained by k-ε model.

4.2. Temperature Distribution

Temperature is the main component for thermal comfort. The information about temperature profile in cubic buildings, as well as computational domain, is provided in this section. Ambient temperature is considered to calculate the temperature distribution. The graphs in Figure 15 display the temperature distribution profile for all (four) cases in Section A, Section B and Section C respectively at

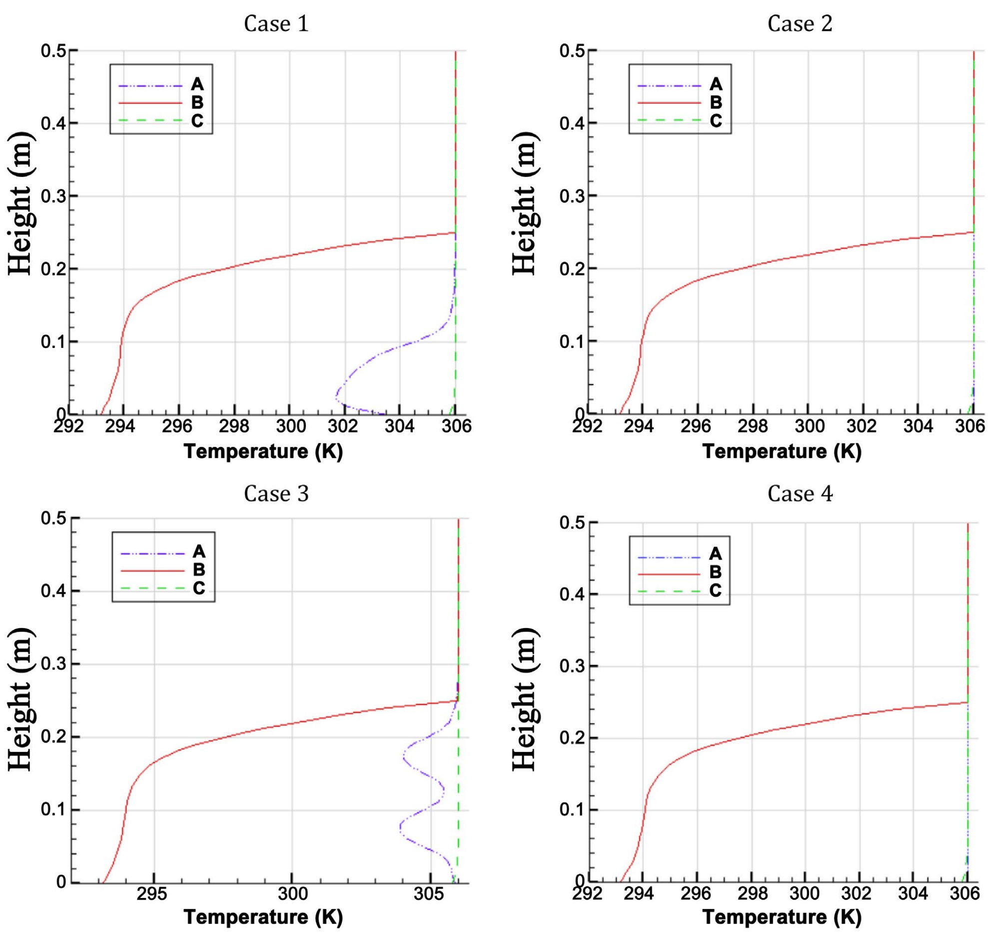

Figure 15. Temperature distribution in Section A (Dash Dot Dot), Section B (Solid line), Section C (Dashed) for all cases at $t = 60$ s.

Table 4. Volume average temperature (K) in the room.

Time (s)	Volume Average Temperature (K)			
	Single Windward	Single Leeward	Double Windward	Double Leeward
43,200	293.1665	293.1817	293.1717	293.1830
43,201	293.9614	293.9601	293.9601	293.9591
43,202	294.3805	294.3702	294.3714	294.3683
43,203	294.7133	294.6976	294.7030	294.6954
43,204	294.9918	294.9746	294.9859	294.9758
43,205	295.2324	295.2186	295.2342	295.2237
43,210	296.1641	296.1692	296.1808	296.1693
43,215	296.8354	296.8679	296.8822	296.8629
43,220	297.3976	297.4266	297.4356	297.4178
43,225	297.8754	297.9106	297.9187	297.8911
43,230	298.2864	298.3428	298.3455	298.3254
43,235	298.6696	298.7319	298.7233	298.7028
43,240	299.0232	299.0795	299.0596	299.0232
43,245	299.3467	299.3837	299.3592	299.3147
43,250	299.6411	299.6594	299.6177	299.5866
43,255	299.9038	299.91069	299.8595	299.8380
43,260	300.1220	300.1409	300.0855	300.0714

time (t) = 3 sec. An interesting observation is that air temperature is fluctuating so much for windward opening(s) (Case 1 and Case 3) in Section A because hot air that exists outside the room is entered easily into the room but the room temperature is comparatively cool. This cold temperature influences the outside temperature when air comes out of the room. From the figure, it is clear that the air temperature fluctuation is decreasing in Section A when time is increasing gradually. For every case, the outside temperature of the room is around 306 K where the minimum and the maximum room temperature is approximately 293 K and 300 K respectively. In all cases, the low temperature is existing in the floor. When time is increasing, the roof of the cubic building is heated gradually for a certain period, which gives rise to the room temperature. However, the ASHRAE Standard 55 [26] states that occupants may feel uncomfortable due to contact with floor surfaces that are too warm or too cool, giving an allowable range of floor temperatures between 292 K and 303 K. In this study, only solar radiation effect is regarded but no other heat source or mechanical system is accounted here. Since room temperature is a vital factor so average volume temperature is needed. **Table 4** shows the details of the average volume temperature for all cases at different times. The average volume temperature for double windward openings and double leeward openings is much closer. At different times, the average volume temperature for double leeward opening is comparatively less than the double windward openings.

4.3. Ventilation Rate

Bangladesh is situated in both the eastern and northern hemispheres. So, wind speed and wind direction is an important part for room temperature. Since this research is time-dependent and also related to solar radiation, so sunlight is necessary. In this study, a clear sunny day at 12:00 pm is considered to calculate ventilation rate for a cubic room that is filled with air. The air flow rate for all cases is shown in Table 5. It is observed that maximum and minimum ventilation rates occur in double windward openings and single leeward opening respectively. From this table, it is clear that double windward openings allow more air to enter into the room than other openings and that's why more ventilation rate is accounted.

Table 5. Ventilation rate.

Time (s)	Velocity Magnitude (m^3/s)			
	Single Windward	Single Leeward	Double Windward	Double Leeward
43,200	1.1186E−3	1.1504E−3	3.2830E−3	3.3590E−3
43,201	2.1524E−3	2.4010E−3	2.4767E−3	2.4714E−3
43,202	1.6644E−3	1.3614E−3	2.7603E−3	1.9632E−3
43,203	1.6735E−3	1.6730E−3	2.7844E−3	1.7178E−3
43,204	1.6844E−3	1.4896E−3	2.7802E−3	1.6179E−3
43,205	1.6856E−3	1.3442E−3	2.7792E−3	1.5709E−3
43,210	1.6825E−3	9.5178E−4	2.7675E−3	1.4756E−3
43,215	1.6863E−3	9.2494E−4	2.7692E−3	1.4625E−3
43,220	1.6895E−3	9.2382E−4	2.7698E−3	1.4611E−3
43,225	1.6898E−3	9.2392E−4	2.7696E−3	1.4630E−3
43,230	1.6891E−3	9.2485E−4	2.7693E−3	1.4657E−3
43,235	1.6882E−3	9.2650E−4	2.7694E−3	1.4652E−3
43,240	1.6876E−3	9.2859E−4	2.7698E−3	1.4636E−3
43,245	1.6873E−3	9.3012E−4	2.7704E−3	1.4639E−3
43,250	1.6875E−3	9.3067E−4	2.7701E−3	1.4643E−3
43,255	1.6880E−3	9.3037E−4	2.7696E−3	1.4643E−3
43,260	1.68914E−3	9.2956E−4	2.7692E−3	1.4639E−3

Air-Change-per-Hour (ACH) value is calculated for each case so that the ventilation findings can be compared with indoor air-quality standards. The ACH value for single windward, single leeward, double windward and double leeward are 6.451, 3.072, 10.368 and 5.606 respectively.

4.4. Radiosity

Radiosity is the summation of the reflected and the emitted radiation. Since all objects except the transparent window are modelled as grey bodies, so radiosity is another parameter which is defined as the rate at which radiation leaves a given surface per unit area. In this study, the lower surface of the computational domain and building are considered as sand and concrete materials, respectively. Figure 16 shows the surface radiosity for all cases of computational domain and a cubic room, respectively. Figures show that the range of the radiosity is 353 to 405 for the room, as well as computational domain at 12:00 pm. In a cubic room, two walls and the floor are free from surface radiosity because these walls are situated in opposite side of the sunlight.

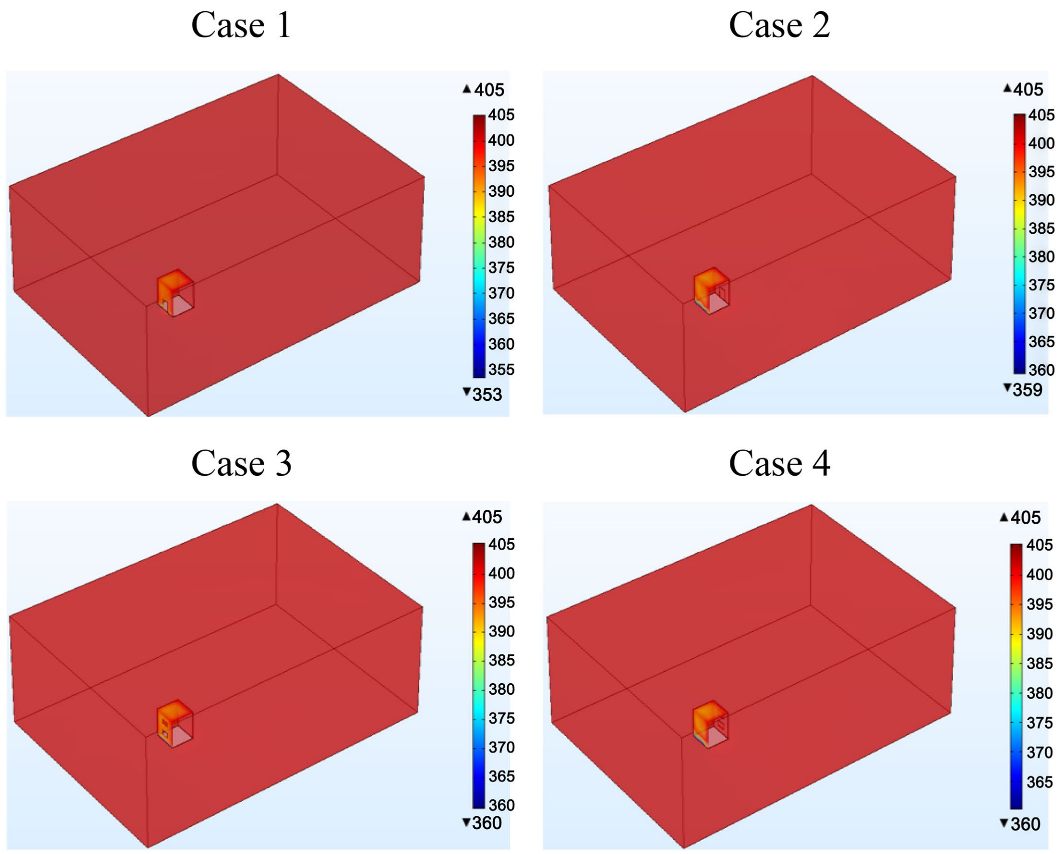

Figure 16. Surface radiosity in computational domain for all cases at $t = 60\ \text{s}$.

The thermal comfort of the occupant within the indoor environment is an important for indoor air quality. Thermal comfort essentially means the condition of mental satisfaction with the thermal environment. In practice, it is not necessary to provide thermal comfort that satisfies each person. Instead, a level of thermal comfort that can satisfy the majority of occupants should be provided. The indoor thermal environment also influences the perception of air quality and can directly or indirectly affect occupant health. Thus, the strategies and methods for maintaining suitable indoor environment conditions, such as indoor air quality and thermal comfort, vary for different locations as well. After the effect of solar radiation, it is clear that in all cases, air temperature inside the room maintains the ASHRAE [26] standard in the context of the weather in Dhaka city.

5. Conclusions

CFD modeling is a very useful tool in natural ventilation design. It enables designers to analyze various designs and evaluate the abilities of these designs before beginning actual implementation of them. However, since CFD has been used for some approximations to determine the flow, it is also very important, therefore, to ensure that it is applied accurately. This is especially true for the case of natural ventilation, which is characterized by unpredictable and complicated airflow patterns and presents a challenge to the field of CFD modeling. The CFD tool has therefore been validated solely for the purpose of natural ventilation study. The results were compared with one empirical model of double window openings setup for steady state single-sided ventilation from the literature. The performance of CFD for these validation cases has been very good and promising overall.

The natural ecosystem is impacted by climatic changes. Air pollution and climate changes are closely related. Global warming occurs due to many reasons, but air pollution is one of them. Communities can preserve air quality by minimizing the sources of air pollution.

- The distribution of the airflow velocity inside and around the building, as well as the ventilation rate, has been calculated.
- All the results have been compared with the experimental data, which were provided in references.
- The information about the air flow rate, flow pattern and temperature distribution is provided to observe the impact of solar radiation on natural ventilation.
- In all cases, air velocity and temperature inside the room maintain the ASHRAE standard.
- By the basis of air quality and the volume average temperature, it can be concluded that double openings in windward wall are more comfortable than the other openings.
- In the context of the weather condition of Dhaka, it would reduce the consumption of mechanical system and build an energy-efficient country.

Acknowledgements

I would like to thank my supervisor Professor Dr. Md. Abdul Hakim Khan and my beloved family.

Conflicts of Interest

The author declares no conflicts of interest regarding the publication of this paper.

References

[1] International Energy Agency (2013) World Energy Outlook 2013.

[2] Kusuda, T. (1977) Fundamentals of Building Heat Transfer. *Journal of Research of the National Bureau of Standards*, **82**, 97-106. https://doi.org/10.6028/jres.082.008

[3] Jiang, Y., Alexander, D., Jenkins, H., Arthur, R. and Chen, Q. (2003) Natural Ventila-

tion in Buildings: Measurement in a Wind Tunnel and Numerical Simulation with Large-Eddy Simulation. *Journal of Wind Engineering and Industrial Aerodynamics*, **91**, 331-353. https://doi.org/10.1016/s0167-6105(02)00380-x

[4] Allocca, C., Chen, Q. and Glicksman, L.R. (2003) Design Analysis of Single-Sided Natural Ventilation. *Energy and Buildings*, **35**, 785-795. https://doi.org/10.1016/s0378-7788(02)00239-6

[5] Jiang, Y. and Chen, Q. (2003) Buoyancy-Driven Single-Sided Natural Ventilation in Buildings with Large Openings. *International Journal of Heat and Mass Transfer*, **46**, 973-988. https://doi.org/10.1016/s0017-9310(02)00373-3

[6] Seifert, J., Li, Y., Axley, J. and Rösler, M. (2006) Calculation of Wind-Driven Cross Ventilation in Buildings with Large Openings. *Journal of Wind Engineering and Industrial Aerodynamics*, **94**, 925-947. https://doi.org/10.1016/j.jweia.2006.04.002

[7] Evola, G. and Popov, V. (2006) Computational Analysis of Wind Driven Natural Ventilation in Buildings. *Energy and Buildings*, **38**, 491-501. https://doi.org/10.1016/j.enbuild.2005.08.008

[8] Larsen, T.S. and Heiselberg, P. (2008) Single-sided Natural Ventilation Driven by Wind Pressure and Temperature Difference. *Energy and Buildings*, **40**, 1031-1040. https://doi.org/10.1016/j.enbuild.2006.07.012

[9] Bangalee, M.Z.I., Lin, S.Y. and Miau, J.J. (2012) Wind Driven Natural Ventilation through Multiple Windows of a Building: A Computational Approach. *Energy and Buildings*, **45**, 317-325. https://doi.org/10.1016/j.enbuild.2011.11.025

[10] Montazeri, H. and Blocken, B. (2013) CFD Simulation of Wind-Induced Pressure Coefficients on Buildings with and without Balconies: Validation and Sensitivity Analysis. *Building and Environment*, **60**, 137-149. https://doi.org/10.1016/j.buildenv.2012.11.012

[11] Idris, A. and Huynh, B.P. (2013) Analysis of Single-Sided Ventilated Room with Different Location of Windows Opening Using CFD. *Congress of Numerical Methods in Engineering*, Bilbao, 25-28 June 2013, 1-17.

[12] Gendelis, S. and Jakovics, A. (2007) Influence of Solar Radiation and Ventilation Conditions on Heat Balance and Thermal Comfort Conditions in Living-Rooms. *Proceedings of* 5 *th Baltic Heat Transfer Conference*, Saint-Petersburg, 19-21 September 2007, 634-643.

[13] Bangladesh Power Development Board (2019) Annual Report 2018-2019.

[14] Ahmmad, M.R. (2014) Statistical Analysis of the Wind Resources at the Importance for Energy Production in Bangladesh. *International Journal of u- and e-Service, Science and Technology*, **7**, 127-136. https://doi.org/10.14257/ijunesst.2014.7.2.12

[15] Hossain, M., Bhuiya, M.R. and Al-Mamun, M.M. (2014) An Analysis of the Temperature Change of Dhaka City. *Proceedings of* 5 *th International Conference on Environmental Aspects of Bangladesh*, Dhaka, 4-5 September 2014, 46-48.

[16] Eftekhari, M.M., Marjanovic, L.D. and Pinnock, D.J. (2003) Air Flow Distribution in and around a Single-Sided Naturally Ventilated Room. *Building and Environment*, **38**, 389-397. https://doi.org/10.1016/s0360-1323(02)00016-1

[17] Ayad, S.S. (1999) Computational Study of Natural Ventilation. *Journal of Wind Engineering and Industrial Aerodynamics*, **82**, 49-68. https://doi.org/10.1016/s0167-6105(98)00210-4

[18] Chen, Q. and Srebric, J. (2000) Application of CFD Tools for Indoor and Outdoor Environment Design. *International Journal on Architectural Science*, **1**, 14-29.

[19] Sharma, A. (2021) Introduction to CFD: Development, Application, and Analysis. In:

Introduction to Computational Fluid Dynamics, Springer, 19-33. https://doi.org/10.1007/978-3-030-72884-7_2

[20] Gan, G. (2000) Effective Depth of Fresh Air Distribution in Rooms with Single-Sided Natural Ventilation. *Energy and Buildings*, **31**, 65-73. https://doi.org/10.1016/s0378-7788(99)00006-7

[21] Visagavel, K. and Srinivasan, P.S.S. (2009) Analysis of Single Side Ventilated and Cross Ventilated Rooms by Varying the Width of the Window Opening Using CFD. *Solar Energy*, **83**, 2-5. https://doi.org/10.1016/j.solener.2008.06.004

[22] Chen, Q. (2004) Using Computational Tools to Factor Wind into Architectural Environment Design. *Energy and Buildings*, **36**, 1197-1209. https://doi.org/10.1016/j.enbuild.2003.10.013

[23] Spengler, J.D., Samet, J.M. and McCarthy, J.F. (2001) Chap. 59. Indoor Air Quality Handbook. In: Chen, Q. and Glicksman, L.R., Eds., *Application of Computational Fluid Dynamics for Indoor Air Quality Studies*, McGraw-Hill, 16-17.

[24] Yakhot, V., Orszag, S.A., Thangam, S., Gatski, T.B. and Speziale, C.G. (1992) Development of Turbulence Models for Shear Flows by a Double Expansion Technique. *Physics of Fluids A*: *Fluid Dynamics*, **4**, 1510-1520. https://doi.org/10.1063/1.858424

[25] Rahman, M.H. and Islam, A.K.M.S. (2010) CFD Modelling of Natural and Forced Ventilation System in a Conventional Kitchen in Bangladesh. *The* 13*th Asian Congress of Fluid Mechanics*, Dhaka, 17-19 December 2010, 460-464.

[26] ASHRAE (2010) ASHRAE Standard 55-2010. Thermal Environment Standards for Human Occupancy.